

**Proceedings of PVP2006-ICPVT-11
2006 ASME Pressure Vessels and Piping Division Conference
July 23-27, 2006, Vancouver, BC, Canada**

PVP2006-ICPVT-11-93569

AN ALTERNATIVE METHOD TO THAT OF THE R6 PROCEDURE FOR THE TREATMENT OF COMBINED PRIMARY AND SECONDARY LOADING

D G Hooton, J K Sharples and S F Yellowlees

Serco Assurance, Birchwood Park, Warrington, WA3 6GA, UK

C T Watson

Rolls-Royce plc. Derby, PO Box 2000, DE21 7XX, UK

Permission to reproduce may be sought in writing from the
Commercial Manager, Serco Assurance, Thomson House, Birchwood Park, Risley, Warrington, Cheshire, WA3 6GA, United Kingdom

ABSTRACT

An alternative definition for the assessment point parameter K_r of the R6 defect assessment procedure is proposed, for combined primary and secondary loading. This alternative definition removes the requirement to calculate a plasticity correction factor for secondary stresses, ρ (or V), used in the conventional R6 definition of K_r . To compare these definitions, both the R6 procedure and the alternative method are presented as Crack Driving Force (CDF) estimation schemes. The required inputs to these estimation schemes have been determined from finite element analyses, for the particular case, of a thick-walled cylinder with a fully circumferential internal defect and subjected to internal pressure and a radial through-wall temperature gradient. Comparisons of CDF estimates with those determined from full inelastic finite element analyses have shown, for the cases studied, that both the R6 and alternative approaches provide conservative estimates of CDF compared to those obtained from finite element analyses, with the degree of conservatism far greater for the conventional R6 approach. Further finite element validation with different geometries, loadings and material properties is required before the alternative procedure could be considered for inclusion in the R6 defect assessment procedure as an alternative to the procedure of the main section of the document.

INTRODUCTION

The R6 defect assessment procedure [1] defines failure¹, of a cracked component, by the co-occurrence of the assessment point ($L_r K_r$) and the Failure Assessment Diagram (FAD), $K_r = f(L_r)$, where the assessment point parameters, L_r and K_r , are measures of proximity to failure by plastic collapse and linear elastic fracture mechanics (LEFM), respectively. The K_r parameter is simply the ratio

of the value of the LEFM stress intensity factor to material toughness, and in the case of loading by primary stresses acting alone, a plasticity correction is applied to stress intensity factor through the FAD. For the treatment of combined primary and secondary loading, since secondary stresses are not included in the FAD function $f(L_r)$, a plasticity correction factor ρ (or V) is applied to the secondary stress component of the K_r parameter. Two procedures for the evaluation ρ (or V) are presented in R6: a simplified conservative method for moderate levels of secondary stress; and a general more detailed method which requires the use of 'Look-up' tables.

In this paper a single, simple to apply and less conservative alternative procedure is proposed, which removes the need to calculate ρ (or V) factors, and hence does not require the use of 'Look-up' tables. Both the detailed R6 and the alternative procedures are compared with results from inelastic finite element analyses, in terms of crack driving forces (CDF). First, methods based on the R6 procedures, for the estimation of CDF for combined primary and secondary loading, are outlined. The alternative simpler method for the estimation of CDF is then developed, based on the treatment of combined loading in the Time-Dependent Failure Assessment Diagram (TDFAD) approach of the R5 [2] assessment procedure for the high temperature response of structures. Finite element analyses are then described for the calculation of CDF for a fully circumferential internal defect in a thick-walled cylinder, subjected to internal pressure and a radial through-wall temperature gradient.

In general, the required inputs to R6 estimates of CDF, elastic stress intensity factors and limit load solutions, are obtained from compendia contained within the R6 document, and advice is also provided in R6 on methods for the calculation of the inelastic stress intensity solution for secondary stresses acting alone, K_J^s , which is a key

¹ Here the term failure is used to define a limiting or unsafe condition, which is a conservative estimate of the actual predicted component failure.

parameter in assessments involving primary and secondary stresses. In this study, inputs to the two CDF estimation schemes have been calculated by finite element analysis. Thus any differences between results for CDF from the two estimation schemes and those from full inelastic finite element analysis, for combined loading, arise from the procedures themselves and not from the inputs to the procedures.

R6 PROCEDURE

The R6 procedure defines failure, of a cracked component under primary loading, by the co-incidence of the assessment point (L_r , K_r) and the Failure Assessment Diagram (FAD), $K_r = f(L_r)$, which has a cut-off at

$L_r^{\max} = \bar{\sigma} / \sigma_y$, where $\bar{\sigma}$ is the material flow stress and σ_y is the yield stress. (see Fig. 1). Three functions for FAD are provided [1], Options 1, 2 and 3 with increasing levels of accuracy, but the same the cut-off is applied for all options.

The coordinates of the assessment point (L_r , K_r) are given by

$$L_r = \frac{\sigma_{\text{ref}}^p}{\sigma_y} \quad (1)$$

where the reference stress for primary loading,

$$\sigma_{\text{ref}}^p = \frac{P}{P_L} \sigma_y, \quad P \text{ is the applied load and } P_L \text{ is the limit load}$$

evaluated for a yield stress σ_y (taken as the 0.2% proof stress),

$$\text{and} \quad K_r = \frac{K_I^p}{K_{\text{mat}}} \quad (2)$$

where K_I^p is the elastic stress intensity factor and K_{mat} is the material fracture toughness. i.e. L_r is a measure of proximity to plastic collapse and K_r is a measure of proximity to LEM failure.

At failure, the applied driving force, K_J , is equal to K_{mat} and the assessment point is coincident with the FAD, $K_r = f(L_r)$.

Hence, from Equation (1)

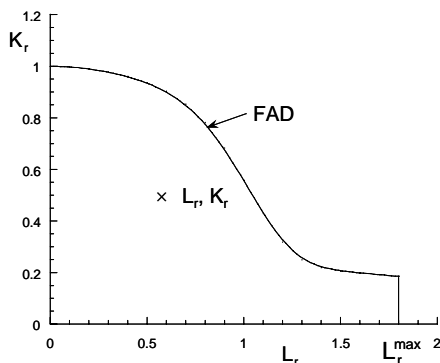


Figure 1 - R6 Failure Assessment Diagram with Assessment Point (L_r , K_r)

$$K_J = \frac{K_I^p}{f(L_r)} \quad (3)$$

which also has a cut-off at L_r^{\max} . i.e. for primary loading only, the R6 procedure [1] effectively uses a FAD to apply a plasticity correction to the elastic value of crack driving force.

The treatment of secondary stress within R6 is based on the work of Ainsworth [3] as subsequently extended by Hooton and Budden [4]. Since the R6 procedures, as described above, are based on reference stress approaches for primary loading only, for combined primary and secondary loading it is necessary to define an equivalent primary reference stress which produces the same crack driving force, K_J , as that for combined loading. The relationship between this equivalent reference stress, σ_{ref} , and reference stresses

σ_{ref}^p and σ_{ref}^s , for primary and secondary loadings, respectively, is shown in Figure 2, taken from [3]. The curves in Figure 2 have been derived from a deformation bounding theorem to give an upper estimate of σ_{ref} . All curves have a maximum value of σ_{ref} corresponding to the L_r^{\max} cut-off of the FAD. i.e. $(\sigma_{\text{ref}})_{\text{max}} = \bar{\sigma}$.

The determination of the crack driving force, K_J , for combined loading in terms of σ_{ref} then proceeds as follows.

The stress intensity factor for combined loading, corresponding to the reference stress, σ_{ref} , may be expressed as

$$K_I = \sigma_{\text{ref}} (\pi a)^{1/2} \quad (4)$$

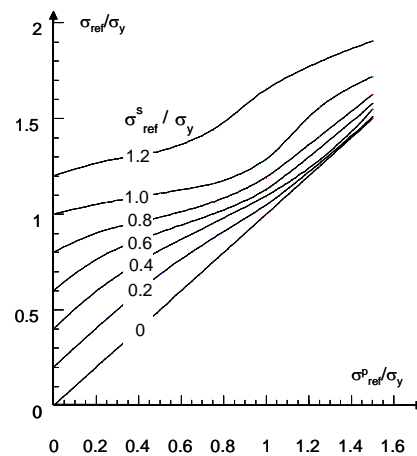


Figure 2 - Definition of Reference Stress under Combined Loading

where \bar{a} is a geometrical parameter which, by assuming σ_{ref} and $\sigma_{\text{ref}}^{\text{p}}$ stress distributions are similar, may be determined from the stress intensity factor for primary loading acting alone, K_{I}^{p} . i.e.

$$K_{\text{I}}^{\text{p}} = \sigma_{\text{ref}}^{\text{p}} (\pi \bar{a})^{1/2} \quad (5)$$

Hence, using the R6 definition of failure, assessment points at failure, described in terms of σ_{ref} , lie on the curve,

$$\frac{K_{\text{I}}}{K_{\text{mat}}} = \frac{\sigma_{\text{ref}} (\pi \bar{a})^{1/2}}{K_{\text{mat}}} = f\left(\frac{\sigma_{\text{ref}}}{\sigma_{\text{Y}}}\right) \quad (6)$$

and from Equations (4), (5) and (6), with the condition at failure $K_{\text{mat}} = K_{\text{J}}$,

$$K_{\text{J}} = \frac{\sigma_{\text{ref}}}{\sigma_{\text{ref}}^{\text{p}}} \frac{K_{\text{I}}^{\text{p}}}{f(L_{\text{r}})} \quad (7)$$

where L_{r} is now defined as $L_{\text{r}} = \sigma_{\text{ref}} / \sigma_{\text{y}}$.

In order to determine σ_{ref} , from Figure 2, it is first necessary to determine values of the primary and secondary reference stresses, $\sigma_{\text{ref}}^{\text{p}}$ and $\sigma_{\text{ref}}^{\text{s}}$, respectively. The first of these, $\sigma_{\text{ref}}^{\text{p}}$, is obtained directly from Equation (1), with the limit load P_{L} determined by finite element analysis or from standard limit load solutions.

In order to evaluate $\sigma_{\text{ref}}^{\text{s}}$ it may be noted that, for secondary loading acting alone, σ_{ref} is equal to $\sigma_{\text{ref}}^{\text{s}}$ and at failure K_{mat} is equal to K_{J}^{s} , the crack driving force for secondary stresses acting alone. (Note: K_{J}^{s} is a key parameter in the determination of K_{J} and various methods for its estimation, rather than calculation by finite elements are described in R6[1].)

Substitution of these conditions into Equation (6) gives

$$\frac{\sigma_{\text{ref}}^{\text{s}} / \sigma_{\text{y}}}{f(\sigma_{\text{ref}}^{\text{s}} / \sigma_{\text{y}})} = \frac{K_{\text{J}}^{\text{s}}}{\sigma_{\text{y}} (\pi \bar{a})^{1/2}} \quad (8)$$

where it has been assumed [3] that the function $f(\sigma_{\text{ref}}^{\text{s}} / \sigma_{\text{y}})$ is given by the R6 Option 1 FAD², $f_1(L_{\text{r}})$.

² In [3] the Option 1 FAD was taken from R6 Revision 3 (1986). However, differences between the Revision 3 FAD and the present Revision 4 FAD are small, and any discrepancies in results from the present analyses arising from the use of the Revision 3 FAD for the derivation of σ_{ref} are insignificant.

i.e.

$$f(\sigma / \sigma_{\text{y}}) = f_1(L_{\text{r}}) = \left[1 + 0.5(\sigma / \sigma_{\text{y}})^2\right]^{-1/2} \times \left[0.3 + 0.7 \exp(-0.6(\sigma / \sigma_{\text{y}})^6)\right] \quad (9)$$

Note also that the cut-off in $f_1(L_{\text{r}})$ at $L_{\text{r}} = L_{\text{r}}^{\text{max}}$ produces a cut-off in Equation (8) at $\sigma_{\text{ref}}^{\text{s}} = \bar{\sigma}$.

Hence, knowing values of $\sigma_{\text{ref}}^{\text{p}}$ and $\sigma_{\text{ref}}^{\text{s}}$, values of σ_{ref} may be determined from the relationships illustrated in Figure 2, and crack driving force may be evaluated from Equation (7).

In R6[1], the treatment of plasticity arising from secondary stress has traditionally been in terms of an interaction parameter ρ , such that

$$K_{\text{r}} = \frac{K_{\text{I}}^{\text{p}} + K_{\text{I}}^{\text{s}}}{K_{\text{mat}}} + \rho \quad (10a)$$

or more recently in terms of a V factor, such that

$$K_{\text{r}} = \frac{K_{\text{I}}^{\text{p}} + VK_{\text{I}}^{\text{s}}}{K_{\text{mat}}} \quad (10b)$$

The definitions of ρ and V are based on the same underlying approach and produce identical results for K_{r} . Therefore, for brevity, only the calculation of the ρ factor is presented here.

From the R6 FAD, $K_{\text{r}} = f(L_{\text{r}}) = f(\sigma_{\text{ref}}^{\text{p}} / \sigma_{\text{y}})$, and Equation (10a) may be expressed as

$$\frac{K_{\text{I}}^{\text{p}}}{K_{\text{mat}}} + \frac{K_{\text{I}}^{\text{s}}}{K_{\text{mat}}} + \rho = f(\sigma_{\text{ref}}^{\text{p}} / \sigma_{\text{y}}) \quad (11)$$

and from Equations (5) and (6)

$$\frac{K_{\text{I}}^{\text{p}}}{K_{\text{mat}}} = \frac{f(\sigma_{\text{ref}}^{\text{p}} / \sigma_{\text{y}})}{\sigma_{\text{ref}}^{\text{p}} / \sigma_{\text{y}}} \cdot \sigma_{\text{ref}}^{\text{p}} / \sigma_{\text{y}} \quad (12)$$

Also, noting that $K_{\text{I}}^{\text{s}} = (K_{\text{I}}^{\text{s}} / K_{\text{J}}^{\text{s}}) K_{\text{J}}^{\text{s}}$, then from Equations (6) and (8)

$$\frac{K_{\text{I}}^{\text{s}}}{K_{\text{mat}}} = \frac{f(\sigma_{\text{ref}}^{\text{s}} / \sigma_{\text{y}})}{\sigma_{\text{ref}}^{\text{s}} / \sigma_{\text{y}}} \cdot \frac{\sigma_{\text{ref}}^{\text{s}} / \sigma_{\text{y}}}{f(\sigma_{\text{ref}}^{\text{s}} / \sigma_{\text{y}})} \cdot \frac{K_{\text{J}}^{\text{s}}}{K_{\text{J}}^{\text{s}}} \quad (13)$$

and substitution from Equations (12) and (13) into Equation (11) gives

$$\rho = \psi + \phi \left(1 - \frac{K_{\text{I}}^{\text{s}}}{K_{\text{J}}^{\text{s}}}\right) \quad (14)$$

where

$$\psi = f\left(\frac{\sigma_{ref}^p}{\sigma_y}\right) - \frac{f\left(\frac{\sigma_{ref}}{\sigma_y}\right) \left[\frac{\sigma_{ref}^p}{\sigma_y} + \frac{\sigma_{ref}^s}{\sigma_y} \right]}{\frac{\sigma_{ref}}{\sigma_y} f\left(\frac{\sigma_{ref}^s}{\sigma_y}\right)} \quad (15)$$

and
$$\phi = \frac{f\left(\frac{\sigma_{ref}}{\sigma_y}\right) \frac{\sigma_{ref}^s}{\sigma_y}}{\frac{\sigma_{ref}}{\sigma_y} f\left(\frac{\sigma_{ref}^s}{\sigma_y}\right)} \quad (16)$$

where again the functions $f(\sigma/\sigma_y)$, (i.e. $f(\sigma_{ref}/\sigma_y)$, $f(\sigma_{ref}^p/\sigma_y)$ and $f(\sigma_{ref}^s/\sigma_y)$), may be taken as the R6 Option 1 FAD, Equation (9).

Functions ψ and ϕ are shown graphically in Figure 3, and are obtained in R6[1] from 'Look-up' tables, in terms of the parameters L_r and $(K_J^s/(K_I^p/L_r))$. Although the functions have been derived using an Option 1 FAD, it is stated [1] that values are not particularly sensitive to the shape of the FAD. It may also be noted, from Equations (1), (5) and (8) that

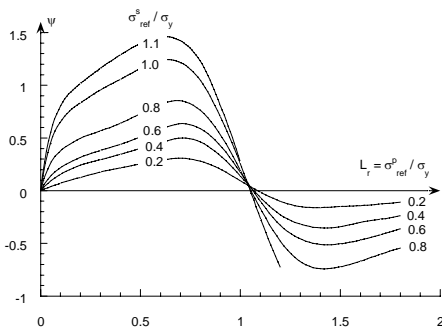


Figure 3a – Dependence of function ψ on the magnitude of primary and secondary stresses.

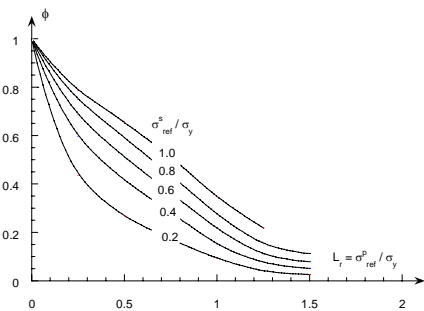


Figure 3b – Dependence of function ϕ on the magnitude of primary and secondary stresses.

the parameter $(K_J^s/(K_I^p/L_r))$ is a function of secondary stress only, and is given by

$$\frac{K_J^s}{K_I^p/L_r} = \frac{\sigma_{ref}^s/\sigma_y}{f(\sigma_{ref}^s/\sigma_y)} \quad (17)$$

To derive crack driving force, K_J in terms of the ρ factor, it is again noted that at failure, the assessment point is coincident with the FAD. i.e. $K_{mat} = K_J$.

Hence, from Equation (10a),

$$K_r = \frac{K_I^p + K_I^s}{K_J} + \rho = f(L_r) \quad (18)$$

to give
$$K_J = \frac{K_I^p + K_I^s}{f(L_r) - \rho} \quad (19)$$

where L_r has the standard R6[1] definition of Equation (1).

From Equations (14) and (19), crack driving force may then be described by the equation

$$K_J = \frac{K_I^p + K_I^s}{f(L_r) - \psi + \phi(K_I^s/K_J^s - 1)} \quad (20)$$

Thus the required inputs for the evaluation of K_J are K_I^p , K_I^s , K_J^s and $L_r(P_L)$, with $f(L_r)$ derived from any of the three FAD options of R6[1].

ALTERNATIVE METHOD

A simpler approach for the determination of σ_{ref} , and hence K_J by Equation (7), may be derived from methods used for combined primary and secondary loading in the Time Dependent Failure Assessment Diagram (TDFAD) procedure of R5 Volume 4/5 Appendix A5 [2]. Details of the derivation and application of these methods are given in [5-6].

Adopting this approach allows K_J to be defined explicitly in terms of K_J^s , and removes the need for the calculation of a ρ factor. Hence, no 'Look-up' tables are required for the determination of the ψ and ϕ parameters.

In consideration of high temperature crack growth, K_r for combined primary and secondary loading is defined [2] by the equation

$$K_r = \frac{\left\{ (K_I^p)^2 [E \epsilon_{ref} / L_r \sigma_{0.2}^c] + (K_I^s)^2 + 2K_I^p K_I^s \right\}^{1/2}}{\left[E \epsilon_{ref} / L_r \sigma_{0.2}^c \right]^{1/2} K_{mat}^c} \quad (21)$$

where $L_r = \sigma_{ref}^p / \sigma_{0.2}^c$, $\sigma_{0.2}^c$ is the 0.2% proof stress from the isochronous stress-strain curve, ϵ_{ref} is the total strain at the stress $L_r \sigma_{0.2}^c$, and K_{mat}^c is a time dependent material toughness.

In the absence of creep effects, $\sigma_{0.2}^c = \sigma_y$, $K_{mat}^c = K_{mat}$, and $L_r = \sigma_{ref}^p / \sigma_y$. Also the R6 Option 2 FAD, (see Equation (31)), apart from the minor correction for small scale yielding, can be expressed as

$$f(L_r) = [E\varepsilon_{ref} / \sigma_{ref}]^{-1/2} \quad (22)$$

Hence,

$$K_r = \frac{f(L_r)}{K_{mat}} \left\{ \left(\frac{K_I^p}{f(L_r)} \right)^2 + (K_I^s)^2 + 2K_I^p K_I^s \right\}^{1/2} \quad (23)$$

and at failure defined by points on the FAD, $K_r = f(L_r)$ and $K_{mat} = K_J$, to give

$$K_J = \left\{ \left(\frac{K_I^p}{f(L_r)} \right)^2 + (K_I^s)^2 + 2K_I^p K_I^s \right\}^{1/2} \quad (24)$$

If σ_{ref}^s is defined in the manner of [3], i.e. replacing K_J^s by K_I^s in Equation (8),

$$\frac{\sigma_{ref}^s}{\sigma_y} = \frac{K_I^s}{K_I^p} f\left(\frac{\sigma_{ref}^s}{\sigma_y}\right) \frac{\sigma_{ref}^p}{\sigma_y} \quad (25)$$

then Equation (24) for K_J , assuming that the reference length for secondary and combined loading is that for primary loading (\bar{a} of Equation (5)), may be expressed as [6]

$$\frac{\sigma_{ref}}{\sigma_y} = f\left(\frac{\sigma_{ref}}{\sigma_y}\right) \left\{ \left[\frac{\sigma_{ref}^p / \sigma_y}{f(\sigma_{ref}^p / \sigma_y)} \right]^2 + \left[\frac{\sigma_{ref}^s / \sigma_y}{f(\sigma_{ref}^s / \sigma_y)} \right]^2 + \frac{2\sigma_{ref}^p \sigma_{ref}^s / \sigma_y^2}{f(\sigma_{ref}^p / \sigma_y)} \right\}^{1/2} \quad (26)$$

which is shown in Figure 4. It is seen that Figure 4, although derived from consideration of elastic-creep behaviour, exhibits the same trends in relationships between σ_{ref} , σ_{ref}^p and σ_{ref}^s as shown in Figure 2, and both σ_{ref} and σ_{ref}^s again have cut-offs at the flow stress $\bar{\sigma}$. It may also be noted that Equation (26) can be solved for σ_{ref} by using the 'Goal Seek' tool in an Excel spreadsheet or an equivalent solver.

In the derivation of Figure 4, the functions $f(\sigma_{ref}^s / \sigma_y)$ and $f(\sigma_{ref}^p / \sigma_y)$ in Equations (25) and (26) are again assumed to have the same form as the Option 1 FAD, Equation (9).

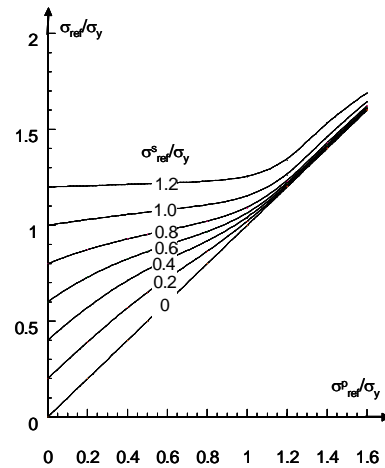


Figure 4 – Definition of reference stress under combined loading (TDFAD approach)

For consistency with the present R6 procedures [1], it may be noted that, in view of Equation (26), ρ factors, based on the relationships of Figure 4, could be calculated directly, as functions of $K_J^s / (K_I^p / L_r)$ and L_r , from Equations (5), (8), (14), (15), (16) and (26), and 'Look-up' tables provided for the determination of ψ and ϕ factors as in R6[1]. However, adopting the present approach there is no requirement to use ρ factors in the calculation of K_J .

If σ_{ref}^s is defined in terms of K_J^s in the manner of [4] then Equation (25) becomes

$$\frac{\sigma_{ref}^s}{\sigma_y} = \frac{K_J^s}{K_I^p} f\left(\frac{\sigma_{ref}^s}{\sigma_y}\right) \frac{\sigma_{ref}^p}{\sigma_y} \quad (27)$$

and Equation (24) becomes

$$K_J = \left\{ \left(\frac{K_I^p}{f(L_r)} \right)^2 + (K_J^s)^2 + 2K_I^p K_J^s \right\}^{1/2} \quad (28)$$

Hence, K_J can be derived directly from Equation (28) without requiring 'Look-up' tables for ψ and ϕ factors, and it can be seen that K_J is independent of K_I^s . It is also seen from Equation (28) that in the absence of primary stress, $K_J = K_J^s$, and in the absence of secondary stress $K_J = K_I^p / f(L_r)$, which is Equation (3). As previously for Equation (20), the required inputs for the evaluation of K_J are K_I^p , K_I^s , K_J^s and L_r , with $f(L_r)$ any of the three FAD options of R6[1]. Also, compared to Equation (20), since ψ and ϕ factors are not required, the influence of the Option 1 FAD on values of K_J is removed, when higher options are used.

Alternatively, for the calculation of values of K_J , σ_{ref}^s may be obtained from Equation (27) using the 'Goal Seek' tool in an Excel spreadsheet or an equivalent solver, and σ_{ref} similarly obtained from Equation (26). K_J may then be derived from the equation

$$K_J = \frac{\sigma_{ref}}{f(\sigma_{ref} / \sigma_y)} \frac{K_I^p}{\sigma_{ref}^p} \quad (29)$$

which is identical to Equation (7). This equation gives the identical value of K_J as Equation (28).

Equation (29) may also be used to determine K_J using the R6 approach with the equivalent reference stress determined from Figure 2. Values of K_J obtained in this manner will be identical to those obtained using Equation (20).

A most important result which transpires from modifying Equation (23) in the manner of Equation (28) is that, following this alternative approach, the K_r coordinate of the R6 assessment point (L_r, K_r) becomes

$$K_r = \frac{f(L_r)}{K_{mat}} \left\{ \left(\frac{K_I^p}{f(L_r)} \right)^2 + (K_J^s)^2 + 2K_I^p K_J^s \right\}^{1/2} \quad (30)$$

It is seen from Equation (30), that in the absence of secondary stress, $K_r = K_I^p / K_{mat}$, which is Equation (2).

Adopting this alternative approach the L_r coordinate remains as defined by Equation (1). i.e. $L_r = \sigma_{ref}^p / \sigma_y$.

Hence, the assessment point (L_r, K_r) may be compared with the FAD in the same manner as the R6 approach but, most significantly, the determination of the K_r coordinate does not require the calculation of a ρ factor as used in Equation (10a) of the standard R6 approach. This alternative approach, therefore, requires the same basic inputs as the standard R6 procedure, but is far simpler to apply as it does not require the use of 'Look-up' tables.

WORKED EXAMPLE

Finite element analysis

Finite element analyses have been performed using the ABAQUS general purpose finite element program. One symmetric half of a cylinder was modelled using 900 parabolic axisymmetric elements with the smallest elements 100 μ m in size. The cylinder was 1000 mm high cylinder, 100mm thick with 550mm outer radius, and contained a fully circumferential crack at the inner surface of depth 10mm. Material properties were taken as those of SA508 ferritic steel.

The applied primary loading was internal pressure, and secondary loading, consisting of a linear temperature gradient across the wall of the cylinder, was applied with inner and outer surface temperatures of -140°C and 140°C, respectively. This temperature range was selected to give plastic strains at the surfaces of the cylinder, in the absence of pressure, whilst keeping the bulk of the section elastic.

The finite element value of the limit load, $P_L = 94.9$ MPa, was determined as the value of pressure at which the CDF, J , for a perfectly plastic material of yield stress strength, tended to infinity.

Elastic and inelastic values of CDF, J_e and J respectively, were determined for pressure loadings only, with values of pressure up to $1.1 \times P_L$, to give the Option 3 FAD,

$$f_3(L_r) = (J_e / J)^{1/2} = K_I^p / K_J^p \quad (31)$$

In Figure 5, this curve is compared with the Option 1 FAD, Equation (9), and the Option 2 FAD given by

$$f_2(L_r) = \left[\frac{E \epsilon_{ref}}{L_r \sigma_y} + \frac{L_r^3 \sigma_y}{2E \epsilon_{ref}} \right]^{-1/2} \quad (32)$$

with $L_r = P / P_L$ and ϵ_{ref} the strain at a stress $L_r \sigma_y$.

Of the required inputs to Equations (20) and (28), to determine estimates of CDF, values of K_I^p were provided from the pressure loading cases through the relationship $K = \sqrt{JE'}$,

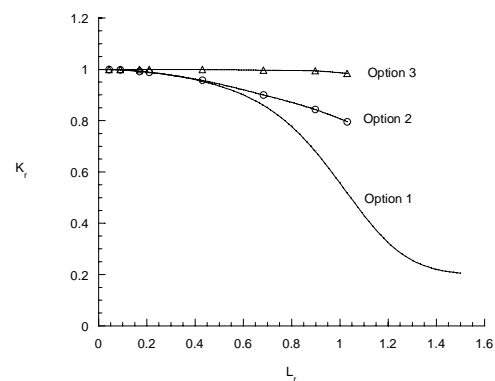


Figure 5 – Comparison of R6 FADs

where $E' = E / (1 - \nu^2)$. Other inputs, elastic and inelastic values of CDF for secondary loading only, K_I^s and K_J^s , respectively, were obtained from the single thermal loading case. Values of the CDF for combined loading, K_J , were

evaluated for the full range of pressure loadings combined with the single thermal loading case.

Estimates of K_J

Estimates of K_J are derived from Equations (20) and (28) with inputs from finite element analysis and the FADs of Equations (9), (32) and (31).

Comparison of results

By determining all inputs to CDF estimation schemes from finite elements analyses, any difference between estimates of K_J and its finite element value arises from the estimation procedure rather than by inputs to the equations.

Comparisons of values of crack driving force with those obtained from estimation procedures are presented in Figure 6, where K_J estimates have been normalised by corresponding finite element values and plotted against the parameter $L_r = P/P_L$. Results based on the R6 and alternative procedures are shown in Figures 6a and 6b, respectively. Clearly, at $L_r = 0$, $K_J = K_J^s$ and all curves start at a K_J ratio of unity. At higher values of L_r , all curves have K_J ratios greater than unity, indicating the conservatism of the methods in all cases.

DISCUSSION OF RESULTS

Differences between the curves of Figures 6a and 6b may be explained in terms of equivalent reference stress and the different FAD options. From Equations (7) and (29), K_J , for both the standard R6 and the alternative method, is given by the equation

$$K_J = \frac{\sigma_{ref} (\pi a)^{1/2}}{f(\sigma_{ref} / \sigma_y)} \tag{33}$$

where $f(\sigma_{ref} / \sigma_y)$ is the curve of any of the options of FAD, shown in Figure 5.

Hence, for a given value of reference stress, the higher the FAD option number the higher the value of the function $f(\sigma_{ref} / \sigma_y)$, from Figure 5, and the lower the value of K_J from Equation (33). A trend which is clearly exhibited in Figure 6, with increasing divergence of the curves with increasing values of L_r , and hence also increasing values of reference stress. It may also be noted from Figures 2 and 4 that, for increasing values of primary and secondary reference stress, higher values of equivalent reference stress are predicted by the approach [3], adopted in R6, compared to present proposals. Therefore, greater deviation from unity is exhibited in Figure 6a compared to Figure 6b, in which values of reference stress are lower for the same value of L_r . It is also clear from Equation (33) that modest increases in reference stress may produce significant increases in values of crack driving force. e.g. it has been

shown that for a value of $L_r = 0.68$, the difference in reference stress between R6 and the alternative method is 7% which produces a 39% difference in the crack driving force value, when using the Option 1 FAD. Therefore, present results indicate that the better estimates of reference stress and hence crack driving force are provided by the alternative method. Although, clearly, much further finite element validation, with different geometries, loadings and material properties is required before the alternative procedure could be considered for inclusion in R6 [1].

CONCLUDING REMARKS

An alternative definition of the R6 assessment point parameter K_r has been proposed, for combined primary and secondary loading. i.e.

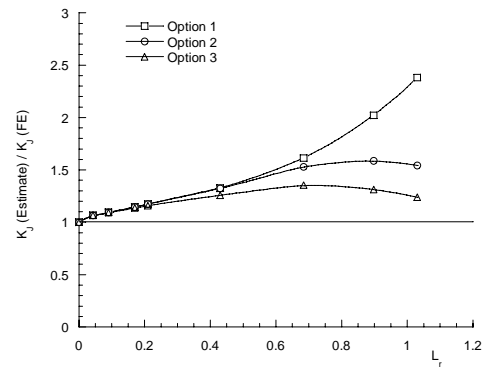


Figure 6a – Comparison of KJ estimates with FE values (R6 Method)

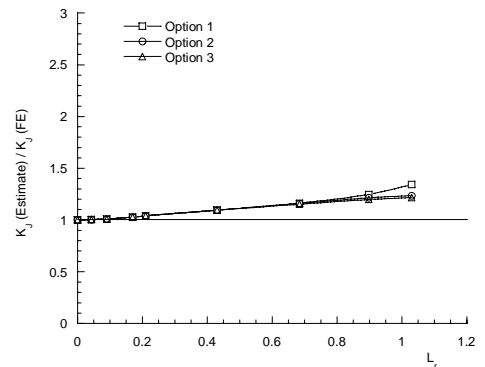


Figure 6b – Comparison of KJ estimates with FE values (Alternative Method)

$$K_r = \frac{f(L_r)}{K_{mat}} \left\{ \left(\frac{K_I^p}{f(L_r)} \right)^2 + (K_J^s)^2 + 2K_I^p K_J^s \right\}^{1/2}$$

where the stress intensity factors and material toughness symbols K have the same definitions as those of R6, and

the function $f(L_r)$ is any of the FAD options of R6. The definition of the L_r parameter remains unchanged. i.e. $L_r = \sigma_{ref}^p / \sigma_y$, where again stresses σ retain their R6 definitions.

This definition of K_r , which is based on the approach for combined loading used in the R5 time-dependent FAD procedure, has the distinct advantage over the conventional R6 approach in that it does not require the determination of a ρ (or V) factor, and hence does not require the use of 'Look-up' tables. It also provides consistency between R6[1] and R5[2] in the definition of reference stress for combined primary and secondary loading.

In order to compare this alternative approach with the conventional R6 approach, finite element analyses have been performed to evaluate crack driving force for a fully circumferential internal defect in a thick-walled cylinder under internal pressure and a radial through-wall temperature gradient. All inputs required for the estimation of crack driving force by both the conventional R6 and the alternative approach have also been determined by finite element analysis. Hence, any differences between estimates of crack driving force and finite element values arise solely from the estimation procedures.

Results for crack driving forces, for a range of applied pressures and a constant value of linear temperature gradient, have shown that both estimation procedures, the conventional R6 approach and the alternative approach, are conservative compared to finite element values, with conservatism increasing with increase in applied pressure and decreasing with the higher the R6 FAD option number used. The degree of conservatism is far greater for the conventional R6 approach, especially at higher values of L_r . The results indicate that the alternative procedure has

considerable potential advantage over the present R6 procedures both in simplifying the application of the procedure and reducing levels of conservatism. Although, clearly, much further finite element validation, with different geometries, loadings and material properties is required before the alternative procedure could be considered for inclusion in the R6 defect assessment procedure.

ACKNOWLEDGEMENTS

This paper is published by permission of Serco Assurance and Rolls Royce plc. The authors would also like to thank Mr H Dodia of Serco Assurance for the provision of finite element calculations.

REFERENCES

- [1] R6: Assessment of the integrity of structures containing defects, British Energy Generation Limited, Revision 4 (2001)
- [2] R5: Assessment procedure for the high temperature response of structures, British Energy Generation Limited, Issue 3 (2003)
- [3] R A Ainsworth, The treatment of thermal and residual stresses in fracture assessments. *Eng. Fract. Mech.*, 24, 65-76, (1986).
- [4] D G Hooton and P J Budden, R6 developments in the treatment of residual stresses. *ASME PVP*, 304, 503-509, (1995).
- [5] R A Ainsworth, The use of a failure assessment diagram for initiation and propagation of defects at high temperatures. *Fatigue Fract Engng Mater Struct* 16:1091-1108 (1993)
- [6] D G Hooton and R A Ainsworth, Failure assessment diagrams for high temperature defect assessment under variable loading conditions. *SMiRT 16*, Washington, (2001).